Biocatalysis, Protein Engineering, and Nanobiotechnology **Biotechnology and Bioengineering**
DOI 10.1002/bit.26071

Continuous multistep synthesis of perillic acid from limonene by catalytic biofilms under segmented flow†

Running Title: Biofilm-based multi-step synthesis of perillic acid

Christian Willrodt[1,*], Babu Halan[1,*], Lisa Karthaus[2], Jessica Rehdorf[3], Mattijs K. Julsing[2], Katja Buehler[1], and Andreas Schmid[1#]

* these authors contributed equally

[1] Department Solar Materials, Helmholtz Centre for Environmental Research (UFZ), Leipzig, Germany

[2] Laboratory of Chemical Biotechnology, Department of Biochemical and Chemical Engineering, TU Dortmund University, Dortmund, Germany

[3] BRAIN Aktiengesellschaft, Zwingenberg, Germany

[#]Correspondence to:
Andreas Schmid
Department Solar Materials, Helmholtz Centre for Environmental Research (UFZ), Permoserstrasse 15, 04318 Leipzig, Germany
telephone: +0049-341-235-1246
fax: +0049-341-23545-1286
email: andreas.schmid@ufz.de

†This article has been accepted for publication and undergone full peer review but has not been through the copyediting, typesetting, pagination and proofreading process, which may lead to differences between this version and the Version of Record. Please cite this article as doi: [10.1002/bit.26071]

Additional Supporting Information may be found in the online version of this article.

Received April 22, 2016; Revision Received July 25, 2016; Accepted August 1, 2016

Abstract

The efficiency of biocatalytic reactions involving industrially interesting reactants is often constrained by toxification of the applied biocatalyst. Here, we evaluated the combination of biologically and technologically inspired strategies to overcome toxicity related issues during the multi-step oxyfunctionalization of (*R*)-(+)-limonene to (*R*)-(+)-perillic acid. *Pseudomonas putida* GS1 catalyzing selective limonene oxidation via the *p*-cymene degradation pathway and recombinant *P. taiwanensis* VLB120 were evaluated for continuous perillic acid production. A tubular segmented-flow biofilm reactor was used in order to relieve oxygen limitations and to enable membrane mediated substrate supply as well as efficient *in situ* product removal. Both *P. putida* GS1 and *P. taiwanensis* VLB120 developed a catalytic biofilm in this system. The productivity of wild-type *P. putida* GS1 encoding the enzymes for limonene bioconversion was highly dependent on the carbon source and reached 34 g L_{tube}^{-1} day^{-1} when glycerol was supplied. More than 10-fold lower productivities were reached irrespective of the applied carbon source when the recombinant *P. taiwanensis* VLB120 harboring *p*-cymene monooxygenase and *p*-cumic alcohol dehydrogenase was used as biocatalyst. The technical applicability for preparative perillic acid synthesis in the applied system was verified by purification of perillic acid from the outlet stream using an anion exchanger resin. This concept enabled the multi-step production of perillic acid, which might be transferred to other reactions involving volatile reactants and toxic end-products.

Keywords: continuous process, biofilm, segmented-flow, multi-step oxyfunctionalization, limonene, perillic acid

This article is protected by copyright. All rights reserved

Introduction

Many interesting reactants for industrially relevant biotransformations can be classified as hydrophobic solvents, which are toxic to the biocatalyst by affecting the cellular viability. This will result in reduced biocatalyst efficiencies and lower reactor productivities in synthetic processes. One of the major challenges in whole cell biocatalysis is overcoming process constraints caused by solvent toxicity (Heipieper et al., 2007; Xue and Woodley, 2012). Solvent toxicity may be counteracted by biologically and/or technologically inspired strategies. Technologically oriented approaches often exploit multiphasic production systems (Lima-Ramos et al., 2014; Straathof, 2003) taking advantage of the enhanced solubility of toxic reactants/products in water immiscible phases, while the whole cell biocatalyst resides in the aqueous environment (Hack et al., 2000; Stark and von Stockar, 2003). The concentration of the respective compound is thus kept below toxic levels in the aqueous biocatalyst environment. Likewise, strategies for controlled substrate supply and continuous product removal can be employed to reduce contact time between the biocatalyst and the toxic product (Hilker et al., 2006; Schewe et al., 2015). Biologically inspired strategies include the utilization of naturally solvent tolerant production strains (Inoue and Horikoshi, 1989). Several *Pseudomonas* species, for instance, feature adaptive mechanisms such as morphological changes, alteration of membrane fluidity, or modification of surface properties to overcome toxic effects of solvents (Heipieper et al., 2007; Segura et al., 2012).

The exploitation of alternative biocatalyst configurations such as resting instead of growing cells or immobilized instead of suspended cells are additional powerful strategies to cope with toxic reactants (Willrodt et al., 2015). Naturally immobilized cells on a surface embedded in a self-produced matrix of extracellular polymeric substances are referred to as biofilms (Costerton et al., 1995). Microbial cells that are immobilized in biofilms are described to exhibit significantly enhanced tolerance towards antimicrobial agents (Costerton et al., 1995) and organic solvents (Halan et al., 2011; Halan et al., 2016; Li et al., 2006). This increased tolerance is often attributed to both physical parameters such as limited exposure of toxic reactants and biological parameters such

as adaptive stress responses, lower metabolic activity, or the formation of persister cells (Stewart, 2002; Walters et al., 2003). Microbial biofilms have a long-lasting success in biological waste water treatment (Qureshi et al., 2005) and bioremediation (Singh et al., 2006), but can also be applied as living biocatalysts in continuous chemical syntheses (Halan et al., 2012).

P. taiwanensis VLB120ΔC, a biofilm forming bacterial strain was cultivated in a segmented flow biofilm reactor set-up and productivities of up to 164 g L_{tube}^{-1} day^{-1} (~46.5 g m^2 d^{-1}) for the one-step synthesis of (*S*)-styrene oxide from styrene were reported. This productivity was achieved by genetically engineering adherence properties of the whole-cell biocatalyst (Schmutzler et al., 2016). Very recently, also the oxyfunctionalization of cyclohexane to cyclohexanol has also been realized in a continuous production system with recombinant *P. taiwanensis* VLB120 (Karande et al., 2016). The application of a biofilm as a catalyst format relieved substrate and product toxicity by using a silicone membrane with dual purpose. The membrane mediated the substrate supply and simultaneously constituted the growth surface.

This work harnesses the advantages of both the biofilm catalyst and the segmented flow-through bioreactor concept for the three-step biooxidation of a readily available volatile monoterpene limonene to the high value but toxic compound perillic acid. Perillic acid is an attractive target for the pharmaceutical and cosmetic industries due to its cytotoxicity to cancer cells (Boon et al., 2000) and its antimicrobial properties (Duelund et al., 2012), respectively. An integrated bioprocess for perillic acid production uses a solvent tolerant *P. putida* GS1 catalyzing limonene oxidation via the native *p*-cymene degradation pathway involving the enzymes CymA, CymB, CymC (Fig. 1B) (Mars et al., 2001; Speelmans et al., 1998). However, this approach still suffered from process instabilities due to toxification of the biocatalyst. *P. putida* GS1 accumulates perillic acid as the sole limonene oxidation product, which cannot be further degraded, due to the lack of an aromatic ring structure, present in the native substrate *p*-cumate. End-product toxification was overcome by solid-liquid extraction of perillic acid using an anion exchange resin (Mirata et al., 2009). We developed a biofilm based process concept as an alternative strategy for overcoming toxicity limitations by

exploiting the catalytic performance of the native strain *P. putida* GS1 and the likewise solvent-tolerant recombinant *P. taiwanensis* VLB120 which has been extensively studied in fine-chemical synthesis (Gross et al., 2010; Gross et al., 2013; Karande et al., 2014; Schmutzler et al., 2015). This optimized process stability during perillic acid production and resulted in the continuous production of perillic acid as the sole oxidation product. The potential to perform multi-step, i.e., multiple consecutive reaction steps catalyzed by individual enzymes, biotransformation in an aqueous-air segmented flow biofilm reactor setup is demonstrated.

Materials & Methods

Chemicals and oligonucleotides. Anhydrous D-(+)-glucose was purchased from Alfa Aesar (Karlsruhe, Germany). Custom synthesized oligonucleotides were purchased from Sigma Aldrich (Steinheim, Germany). All other chemicals were obtained from AppliChem (Darmstadt, Germany), Sigma Aldrich (Steinheim, Germany), or Carl Roth (Karlsruhe, Germany) at the highest purity available.

Bacterial strains and plasmid construction. Wild-type *P. putida* GS1 (DSM 12264) was obtained from the German Collection of Microorganisms and Cell Cultures (DSMZ, Braunschweig, Germany). Cloning of genes was performed by an *in vitro* assembly method (Gibson et al., 2009). Reagents were obtained from Thermo Scientific (Schwerte, Germany). Phusion™ high fidelity polymerase was used according to the manufacturer instructions. *E. coli* DH5α was used for all molecular biology manipulations. Genomic DNA of *P. putida* GS1 was isolated using the peqGOLD Bacterial DNA kit (peqLAB, Erlangen, Germany). The primers were designed on the basis of the available genome sequence of *P. putida* F1 (GenBank ID: CP000712.1). The open reading frames (ORFs) for the cymene monooxygenase *cymAa* and the adjacent reductase *cymAb* were amplified from the genomic DNA using the primers PCW085 (5'-GGAACCAGTAC-TGGAGAATTCCATAATGTGGGAATACATCAAGTAC-3') and PCW086 (5'-ACGGAT-CCCGGGCGCGCCAAGCATACAATTAGCCTTTAGGAGTTCC-3'). PCR settings were set to

40 seconds elongation time and an annealing temperature of 59.1°C. After *Dpn*I treatment of the PCR mix, the 2280 bp amplicon was purified via excision from an agarose gel and subsequently recombined with *Nde*I digested pStyAB-lac (Lindmeyer et al., 2015) leading to the expression plasmid pCom10L:CymA. Expression of the heterologous gene in this vector is driven by the IPTG inducible P_{lacUV5} promotor. The ORF for the *p*-cumic alcohol dehydrogenase (*cymB*) was amplified using PCW093 (5'-AAAGGCTAATTGTATGCTTGG CGCGAGGAGGACAGCTAAATGAGACTGAAAGACAAAGTCG-3') and PCW094 (5'-TCTCTCATCCGCCAAAACAGAAGCTTGAATGTCGTGGCGAATGAC-3'), an annea-ling temperature of 58.6°C and an elongation time of 35 seconds. After *Dpn*I treatment of the PCR mix, the 804 bp amplicon was purified and recombined with digested (*Sgs*I, *Hind*III) pCom10L:CymA resulting in the plasmid pCom10L:CymAB. Accuracy of all manipulations was assessed by sequence analysis. The obtained sequences were identical to the *cymAab* and *cymB* sequences of the *cmt* operon of *P. putida* F1 (GenBank ID: U242215).

Cultivation of bacterial strains. Five mL of lysogeny broth (LB) were inoculated from frozen stocks and incubated for 16 h at 30°C (200 rpm, 2.5 cm amplitude). Five hundred µL from this culture were used to inoculate a 50 mL M9* (Panke et al., 1999) in a 250 mL baffled Erlenmeyer flask preculture supplemented with either 0.5% (w/v) glucose, glycerol or citrate. After overnight incubation at 30°C, this culture was used to inoculate the respective M9* (liquid:gas phase ratio 1:4 in the flask) main cultures at an OD_{450} of 0.2 or the tubular biofilm setup. The cultures for the recombinant strains were supplemented with 50 µg mL^{-1} kanamycin. Gene expression was either induced in the early stationary phase (OD_{450} between 0.6 and 0.8) or, for biofilm applications, already during the M9* preculture.

Analytical procedures. Quantification of the analytes (*R*)-(+)-limonene, (*R*)-(+)-perillyl alcohol, (*R*)-(+)-perillyl aldehyde and (*R*)-(+)-perillic acid (PAc) was performed with a TraceGC Ultra (ThermoFisher Scientific Inc., Waltham, MA, USA) gas chromatography instrument. Nitrogen was applied as a carrier gas and the gas flow rate was set to

1.5 mL min^{-1}. The injector (250°C) was operated in splitless mode. The oven profile was: 80°C (5 min), 80-160°C (7.5°C min^{-1}), 160-300°C (40°C min^{-1}), and 300°C (5 min). Concentrations were determined with standard curves using (*R*)-(+)-limonene, and the (*S*)-enantiomers of perillyl alcohol, perillyl aldehyde, and perillic acid. Standard solutions were prepared in M9* medium and subsequently extracted by the addition of an equal volume of diethyl ether (Et_2O), with 0.2 mM dodecane as an internal standard, and vigorous mixing. The phases were separated by centrifugation (room temperature, 17000 g, 2 min) and the organic phase was dried over anhydrous Na_2SO_4 prior to GC analysis.

The concentrations of glycerol and citrate were assessed by HPLC as described elsewhere (Gross et al., 2010) and cell dry weight in dispersed cultures was calculated from the measured turbidity using the respective conversion factor (LibraS11, Biochrom Ltd., Cambridge, UK, OD_{450} = 1 equals 0.186 and 0.223 g_{cdw} L^{-1} for *P. taiwanensis* VLB120 (Lang et al., 2014) and *P. putida* (Ütkür et al., 2011), respectively).

Limonene toxicity assays. Precultures were incubated as described above. Limonene toxicity was assessed by adding different amounts (0 - 250 mmol L^{-1}) of (*R*)-(+)-limonene directly after inoculation of the main culture (25 mL M9* medium, 250 mL baffled Erlenmeyer flask, 0.5% (w/v) citrate) with M9* overnight cultures of *P. taiwanensis* VLB120 or *P. putida* GS1. In addition to the amounts of limonene added to the aqueous phase, 1 mL of limonene was added to an evaporation container attached to the lid of the flask to saturate the gaseous phase. The flask was sealed tightly to prevent evaporation. Biomass was assessed after 16 h of cultivation at 30°C (after washing twice with 0.1 M potassium phosphate buffer).

Perillic acid toxicity assays. One gram of (*S*)-(-)-perillic acid was dissolved in 4 mL aqueous 2 mol L^{-1} NaOH. The pH was adjusted to 11.5 by adding 10 mol L^{-1} sodium hydroxide and water was added to a final volume of 20 mL. This solution was diluted to the desired 2.5-fold concentrated stock solutions (0 - 150 mmol L^{-1}) with 0.4 mol L^{-1} NaOH. 0.4 mL of these stock solutions were mixed with 0.6 mL M9* medium (1.667-fold concentrated) supplemented with

0.8% (w/v) citrate in a 15 mL cultivation tube. Perillic acid was soluble in alkaline stock solutions and did not precipitate upon dilution with the medium, although the solubility in aqueous systems (~0.8 mmol L^{-1}) was exceeded. Forty µL of a M9* overnight culture of *P. taiwanensis* VLB120 or *P. putida* GS1 were added and biomass was assessed after 16 h of cultivation in a rotary incubator as described above. By preparing appropriate perillic acid stock solutions, the NaOH concentration in the different growth experiments was kept equal to prevent NaOH triggered growth biases. The pH of the M9* medium remained unaltered upon addition of the perillic acid stock solutions.

Resting cell assays. After incubation of *P. taiwanensis* VLB120 harboring either pCom10L:CymA or pCom10L:CymAB in M9* medium with citrate, 1 mM IPTG was added during the early exponential growth phase (OD_{450} of ~0.6) and incubation was continued for 4 h. An aliquot of the cell suspension was centrifuged (4°C, 4618 g, 20 min) and resuspended to 0.6 – 1.2 g_{cdw} L^{-1} in potassium phosphate buffer (0.1 M, pH 7.4). From here, the assays were performed as described elsewhere (Cornelissen et al., 2011).

Biofilm formation capacity. The determination of the biofilm forming capacity was conducted in a tubular reactors setup. M9 minimal medium containing either 0.5% (w/v) glucose, glycerol or citrate was pumped by a peristaltic pump (IPC High Precision Multichannel Dispenser, Ismatec, Wertheim, Germany). Silicon tubes (3 mm inner diameter, 1.5 mm wall thickness, 600 mm length) were used as biofilm surface. Tygon tubes (2.06 mm inner diameter, Tygon R 3607, Ismatec, Wertheim, Germany) were used to connect the bubble traps and the medium reservoirs to the pumps. Prior to inoculation, the reactor was autoclaved and coiled within a flask which was then placed in a 30°C water bath. The reactors were inoculated with respective pre-cultures obtained as described above. The reactor was kept idle for 2 h without any medium flow. Afterwards the medium flow was set to 0.1 ml min^{-1} and operated for 2 days. Biomass was assessed gravimetrically after drying the sample at 85°C. Biofilm biomass was harvested under productive conditions and quantified after 12 days of continuous biofilm cultivation under segmented flow in presence of limonene.

Production of perillic acid in a segmented flow biofilm reactor. For the biofilm-based perillic acid production in principle the same setup as described above was applied, but silicon tubes with an inner diameter of 2 mm, a wall thickness of 1 mm, and a length of 1000 mm were used (0.314 ml reactor volume, Fig. 1A). Additionally, a second peristaltic pump was installed and connected to the system via a T-connector. After 3 days of continuous single phase flow (0.1 ml min^{-1}), air segments were introduced at flow rates of 0.4 ml min^{-1}. 1 mM IPTG was supplied continuously via the feed stream (growth medium). Sterility of the introduced air segments was ensured by installing a syringe filter (0.2 µm, polyether sulfone membrane, VWR, Germany) (Fig. 1A). Upon reactor inoculation, 20 mL (*R*)-(+)-limonene were added to the flask containing the coiled reactor tubing, submerging 20 - 40% of the tubing into limonene. Perillic acid concentrations were assessed after extraction of the reactor outflow with Et_2O at previously defined time points. Dilution rate: 2 h^{-1} (at least 4-5 times higher than the maximum specific growth rate of the strains used).

Purification of perillic acid. Amberlite IRA 410 Cl resin was used to adsorb perillic acid from the reactor outflow as described before (Mirata et al., 2009). Prior to use, the resin was treated with ethanol and water (Mirata et al., 2009). Twelve grams of washed resin were applied to adsorb 80% of the perillic acid from 0.4 L reactor outflow within 4 h of binding. Perillic acid was eluted with a mixture of 4M HCl and ethanol (40:60, volumetric ratio) at 30°C. A second elution step was performed via ethyl acetate treatment. The aqueous and the organic fraction were combined and subjected to distillation in a rotary evaporator to remove ethanol and ethyl acetate. The precipitate was removed by filtration. The filtrate was treated with HCl to precipitate perillic acid.

Results

Recombinant *P. taiwanensis* VLB120 shows high perillic acid formation rates. As the biofilm forming strain *P. taiwanensis* VLB120 is not natively hydroxylating limonene, the respective genes had to be introduced heterologously. The genes for the monooxygenase (CymAa), the respective reductase (CymAb) and the putative *p*-cumic alcohol dehydrogenase (*p*-cumic ADH) were isolated

from the genomic DNA of *P. putida* GS1 and cloned into an expression vector under control of the P_{lacUV5} promoter to construct a *P. taiwanensis* VLB120 capable of perillic acid formation. *P. taiwanensis* VLB120 harbors a variety of alcohol and aldehyde dehydrogenases (Lang et al., 2014). We hypothesized that the additional presence of the *p*-cumic aldehyde dehydrogenase would therefore not be necessary. Resting-cell activity assays have been performed supplying the substrate limonene to resting cells of *P. taiwanensis* VLB120 to verify functional expression of both recombinant genes. Resting cells of *P. taiwanensis* VLB120 harboring the monooxygenase CymA (pCom10L:CymA) showed perillyl alcohol but also perillyl aldehyde and perillic acid formation (Fig. 2**A**). Perillic acid was formed with rather constant rate of approximately 4.5 U g_{cdw}^{-1} upon addition of 2 mM limonene. Apparently, native intrinsic dehydrogenases or CymA itself catalyzed further oxidation to the acid. Coexpression of the *p*-cumic ADH, however, led to increased perillic acid formation (Fig. 2**B**) and doubled the specific production rate.

Although perillic acid was the major product in both cases, perillyl alcohol and aldehyde accumulated to a molar fraction of more than 50% (sum) when only *cymA* was expressed, whereas they constituted less than 10% when *cymA* and *cymB* were expressed simultaneously. In summary, it was verified that functional recombinant expression of the genes *cymA* and *cymB* in *P. taiwanensis* VLB120 was sufficient to produce perillic acid as the major product of limonene oxidation. In order to evaluate its competitiveness with the native production strain *P. putida* GS1 in a microbial perillic acid production process the impact of the reactants on the physiology of *P. taiwanensis* VLB120 and *P. putida* GS1 towards the reactants had to be investigated.

***P. putida* GS1 tolerates higher concentrations of perillic acid and limonene than *P. taiwanensis* VLB120.** Toxicity assays were performed to compare the physiological response of both *P. putida* GS1 and *P. taiwanensis* VLB120 towards limonene and perillic acid. *P. putida* GS1 showed an exceptional tolerance towards the monoterpene limonene (*logP* = 4.46, (Sikkema et al., 1995)). The growth yield of this strain remained unaffected by limonene concentrations as high as 225 mM (Fig.

3**A**). In contrast, the growth of *P. taiwanensis* VLB120 was completely inhibited by limonene concentrations between 50 and 75 mM (Fig. 3**A**). The observed effect might have been due to phase rather than molecular level toxicity as limonene is barely soluble in water (~0.45 mM (Schmid et al., 1992)).

Perillic acid (*logP* = 3.59, predicted, www.chemspider.com) was toxic for both bacterial strains, and growth was completely inhibited in either case at 60 mM. Interestingly, a different profile of perillic acid dependent growth inhibition was observed for *P. taiwanensis* VLB120 as compared to *P. putida* GS1 (Fig. 3**B**). Biomass yields first dropped and then stayed constant between 10 and 35 mM perillic acid for *P. taiwanensis* VLB120 while it continuously dropped in *P. putida* GS1. A similar behavior with respect to the toxicity profile was also observed for the concentration dependent toxicity analysis of perillyl alcohol towards *P. putida* KT2440 (Cornelissen et al., 2011). It is therefore essential to regulate perillic acid concentrations below 35 mM in the aqueous phase for the development of an efficient production process.

Hydroxylation of limonene to perillic acid or perillic acid degradation was not observed with either strain. In *P. putida* GS1 limonene hydroxylation did most likely not occur due a lacking induction of the *cym* gene expression within the experimental time window of the toxicity tests. In conclusion, *P. putida* GS1 is superior in terms of resilience to both limonene and perillic acid as compared to *P. taiwanensis* VLB120. Nevertheless, *P. taiwanensis* VLB120 is a well-characterized biofilm producer and process parameters have been described for the biofilm-based production of toxic compounds such as (*S*)-styrene oxide (Gross et al., 2010; Halan et al., 2011), octanol (Gross et al., 2013), and (*S*)-3-hydroxyisobutyric acid (Lang et al., 2015). Hence, *P. taiwanensis* VLB120 was still included as a potential production strain for perillic acid. The biofilm formation capability of *P. putida* GS1 was unknown and was thus investigated.

Biofilm formation capacity is dependent on the carbon source. In order to investigate whether *P. putida* GS1 is capable of forming biofilms, the strain was cultivated in M9* minimal medium

with glucose, glycerol, or citrate as sole carbon and energy source. These cultures were then used to inoculate a tubular biofilm reactor.

For comparison, the well-characterized biofilm forming strain *P. taiwanensis* VLB120 was cultivated accordingly. The biofilm dry weight was assessed after three days of continuous flow with the respective medium. *P. putida* GS1 formed substantial amounts of biofilms (up to 7 $g_{bdw}\ m_{reactor}^{-2}$, bdw: biofilm dry weight) in the applied setup, independent of the carbon source supplied. In contrast, *P. taiwanensis* VLB120 showed a clear preference for citrate regarding biomass formation (15 $g_{bdw}\ m_{reactor}^{-2}$) (Fig. 4**A**). This preference is in agreement with the specific growth rates during batch cultivation in shake flasks of this strain with the respective carbon sources (data not shown). In conclusion, both strains showed to possess capabilities of biofilm formation producing perillic acid production. Therefore, the two *Pseudomonas* strains were investigated regarding their potential to produce perillic acid in a continuous flow-through system.

Biofilm-based perillic acid production is efficient with *P. putida* GS1 and glycerol as carbon source. Limonene biotransformation into perillic acid by *P. putida* GS1 in a controlled fed-batch reaction setup suffered from a relatively low production time (Mirata et al., 2009). Continuous operation of the reactor would be desirable to this limitation. Therefore, a segmented-flow biofilm reactor setup that allowed for the continuous production of toxic perillic acid was developed (Fig. 1A). The segmented-flow system was harnessed to prevent the limitation of oxygen for both cellular growth and the biocatalytic reaction (Karande et al., 2014).

Both *P. putida* GS1 (Fig. 5A) and *P. taiwanensis* VLB120 (pCom10L:CymAB) (Fig. 5B) cultivated on citrate as sole carbon source, showed very little perillic acid formation during the first two days of cultivation (only aqueous flow, 0.1 mL min^{-1}, 0.5% (w/v) citrate). Perillic acid formation increased after introducing the air flow (0.4 mL min^{-1}) within the next two to three days and reached a plateau productivity value of approximately 5 g $L_{tube}^{-1}\ d^{-1}$ and 2.5 g $L_{tube}^{-1}\ d^{-1}$ for *P. putida* GS1 and *P. taiwanensis* VLB120 (pCom10L:CymAB), respectively. This productivity remained

unaltered high until the experiment was actively terminated 12 days after inoculation. Residual citrate concentrations of more than 4 g L^{-1} were detected at the reactor outlet in either case, indicating that availability of the carbon source did not limit production during steady state operation. The productivity of *P. taiwanensis* VLB120 (pCom10L:CymAB) biofilms for perillic acid formation (max. 2.6 - 3.2 g L_{tube}^{-1} d^{-1}) remained unaffected by changing the carbon source from citrate to glycerol (Fig. 5B). This however did not seem to match the difference in the amount of biomass formed during aqueous phase flow conditions (Fig. 4A) or in segmented flow (Fig. S1). Biomass formation for *P. taiwanensis* VLB120 (pCom10L:CymAB) under productive conditions with citrate as carbon source was doubled as compared to glycerol (14.6 vs. 7.3 g_{bdw} m^2, Fig. S1). SDS-PAGE analyses (Fig. S2) indicated that *cymB* might have been less expressed during biofilm cultivation with citrate.

Interestingly, *P. putida* GS1 cultivated on glycerol produced significantly higher amounts of perillic acid at productivities of up to 15 g L_{tube}^{-1} d^{-1} already during the first two days of cultivation in single aqueous flow. Additional supply of oxygen via air segments initially caused a drop in productivity due to washout of significant amounts of biomass. Afterwards a second generation biofilm was developed. In accordance with that, the productivity increased to a peak of 34 g L_{tube}^{-1} d^{-1} on the eighth day after inoculation and levels at an average productivity of 22 g L_{tube}^{-1} d^{-1} until the end of the experiment (12 days after inoculation). *P. putida* GS1 has formed 2.5-fold higher biomass (biofilm dry weight) with glycerol than with citrate after these 12 days of continuous cultivation.

In conclusion, continuous production of perillic acid is feasible with both wild-type *P. putida* GS1 and recombinant *P. taiwanensis* VLB120 (pCom10L:CymAB) with reasonably high volumetric productivities.

Adaptation of downstream processing yields highly pure perillic acid. Recovery of the reaction product from the fermentation broth is often challenging and hampered by low aqueous product concentrations (Woodley, 2008). The purification of perillic acid has been optimized and reported to profit from a resin-based *in situ* product removal technique with an anion exchanger (Mirata et

al., 2009). Therefore, a portion of the biofilm efflux was collected and the perillic acid was allowed to adsorb to the cationic coating (benzyldimethyl-(2-hydroxyethyl)ammonium) of the resin for 24 h. The adsorbed perillic acid was eluted in two steps using 4 mol L^{-1} HCl/EtOH and ethyl acetate, respectively. After removing the solvent, perillic acid was obtained at a purity of approximately 96% (GC) and an isolation yield of 60%. This finally proves that the biofilm-based production in combination with a potent downstream technique can be utilized for the preparative production of the high value compound perillic acid.

Discussion

Basically, continuous bioproduction processes are desirable for commodity (or bulk) chemical production at industrial scale because of stable productivities, long running-times, and comparatively low operational maintenance requirements (Al-Kaidy et al., 2014). However, the continuous bioproduction of compounds with physicochemical properties (e.g., volatility, toxicity) that do not match with native microbial products is constrained by both biological and technical parameters (Willrodt et al., 2015). These biological and technical features were exploited by applying solvent-tolerant *Pseudomonas* species expressing the perillic acid biosynthesis pathway either natively or recombinantly in a segmented flow biofilm reactor. Both, *P. putida* GS1 and *P. taiwanensis* VLB120 have originally been isolated based on their capability of degrading toxic agents (Speelmans et al., 1998; Panke et al., 1998). *P. putida* GS1 tolerated very high limonene concentrations, but growth was completely inhibited at perillic acid concentrations of 60 mM and higher. *P. taiwanensis* VLB120 was found to be generally more susceptible to both limonene and perillic acid. In contrast to perillic acid, limonene toxicity appeared to be caused by phase toxicity effects. Dissection of the difference between both strains and the underlying mechanisms would require more sophisticated genotypic and phenotypic analyses and was therefore beyond the scope of this study.

The combination of the biocatalyst configuration of naturally immobilized cells and the segmented-flow biofilm reactor were harnessed for continuous perillic acid production and efficient product removal to prevent toxification. The productivity of *P. putida* GS1 for perillic acid production could be increased almost fourfold as compared to the fed-batch process (Mirata et al., 2009), partially as a result of the increased biomass density within the biofilm reactor. However, the comparison of these two systems is biased by the small volumes applied in the biofilm-based production setup. The maximally achieved perillic acid concentrations at the outlet the biofilm reactor is rather low ~5.3 mM and remained below the critical concentration for suspended cells (approximately 39 mM for *P. putida* GS1). Thus, a further increase in productivity seems not yet to be limited by toxicity. However, it has to be noted that local concentrations in the vicinity of the biocatalyst might be significantly higher because the catalytically active biofilm is located close to the silicone membrane.

The productivity of *P. putida* GS1 biofilm cultivated on glycerol is up to six-fold (four-fold after 12 days) higher than the productivity of the same strain cultivated on citrate. This implies that limonene availability and mass transfer were not limiting for the setup on citrate. An increase of the air flow rate to 0.6 mL min^{-1} in the glycerol-based cultivation did not result in a further increase in productivity (data not shown). This indicates that with citrate as carbon source, oxygen mass transfer was not limiting perillic acid production either. However, the 2.5-fold decreased biomass obtained (Fig. S1) with citrate cannot quantitatively reflect the four- to six-fold decrease in productivity. We therefore attribute the increase in productivity to higher expression levels of the genes of the *cym* operon with glycerol as carbon source. This is in accordance to previously published results (Speelmans et al., 1998). It might also be speculated that expression of the *cym* genes is subject to catabolite repression in the presence of organic acids including citrate (Kurbatov et al., 2006; Wolff et al., 1991).

In contrast, perillic acid productivity with the recombinant strain *P. taiwanensis* VLB120 (pCom10L:CymAB) was not affected by the type of the carbon source, although biomass formation

under productive conditions was two-fold higher when citrate was applied as carbon source. A possible explanation could be the putatively reduced expression of *cymB* in the presence of citrate under productive conditions. The overall productivity of *P. taiwanensis* VLB120 (pCom10L:CymAB) is ~10-times lower than the productivity of *P. putida* GS1 during the glycerol-based cultivation, whereas the biomass formation was only fourfold low (Fig. S1). Consequently, the increased performance of *P. putida* GS1 might also be attributed to other factors such as different ratios of cell mass to EPS matrix in biofilms or auxiliary roles of other strain specific enzymes, i.e., other dehydrogenases (CymC) or putative uptake proteins (CymD).

Yet, the achieved concentrations of perillic acid were significantly lower (max. 5.3 mM) compared to the previously reported fed-batch process (Mirata et al., 2009). Here, the small volume of the tubular reactor has to be taken into account and considered as a tunable parameter by retaining the advantages gained from the miniaturization. It seemed logical to increase the catalytically active area simply by enhancing the longitudinal dimension of the tubular bioreactor. The use of a reactor length of 5 m in instead of 1 m for perillic acid production with *P. putida* GS1 cultivated on glycerol, however, resulted in decreased productivities and only a twofold increase in total product amount after 20 days of operation (data not shown). Most likely this can be attributed to an oxygen limitation, which might be overcome by using oxygen enriched air segments.

Traditional strategies for the scale-up of bioprocesses are based on constant k_La values, dimensionless numbers (e.g., Damkoehler number), or geometrical similarities (Marques et al., 2010). In our case, upscaling without losing the miniaturization advantages (diffusion distance, high surface area) might be successful by parallelization (numbering-up) of the tubular setup (Warikoo et al., 2012; Wohlgemuth et al., 2015). In that respect a bundle of only thirty parallel tubes would be required for the production of 100 g perillic acid with *P. putida* GS1 within one month and increasing the cumulative tube volume to one liter would yield more than 1 kg perillic acid. Nevertheless, scale-up of this reactor format by parallelization or numbering-up poses a major challenge with respect to the low product concentrations and comparatively high efflux stream

volumes, which are typical problems in continuous biotechnological syntheses (Stark and von Stockar, 2003). Here, the combination of the continuous perillic acid production with the powerful resin-based *in situ* product removal (Mirata et al., 2009) might partly alleviate these issues. However, the implementation of this technology at industrial scale is rather difficult at this stage and has to be evaluated carefully on a techno-economical basis. It might very well possible, that the low product concentrations obtained in this continuous process require, based on the adsorption isotherm, too high amounts of the adsorbent material making the process inefficient from an economical point of view. Additionally, we have encountered a significant limonene loss of approximately 50% after 12 days of continuous operation due to tube swelling and evaporation via tubing connectors. These issues can be addressed by applying more adequate materials for the growth substratum (e.g., expanded PTFE) and improved reactor design with tube connectors.

In conclusion, the continuous multi-step biotransformation of limonene to perillic acid is possible in a tubular biofilm reactor at comparable productivities achieved for the one-step hydroxylations of cyclohexane (~10 g L_{tube}^{-1} d^{-1}) (Karande et al., 2016) or (S)-styrene oxide (46 g L_{tube}^{-1} d^{-1}) (Karande et al., 2014).

In addition, the product perillic acid could be recovered and purified for potential further applications. Thus, this biofilm reactor concept may be transferred to other reactions involving volatile reactants and toxic end-products to perform efficient preparative multi-step biocatalysis.

Acknowledgements

The authors appreciate Rohan Karande for valuable discussions and important input to the present manuscript. Support with infrastructure of TU Dortmund University at the former Laboratory of Chemical Biotechnology is gratefully acknowledged by CW, BH, KB, and AS.

References

Al-Kaidy H, Duwe A, Huster M, Muffler K, Schlegel C, Sieker T, Stadtmüller R, Tippkötter N, Ulber R. 2014. Biotechnologie und Bioverfahrenstechnik - Vom ersten Ullmanns Artikel bis hin zu aktuellen Forschungsthemen. *Chemie Ing Tech* **86**:2215–2225.

Boon PJ, van der Boon D, Mulder GJ. 2000. Cytotoxicity and biotransformation of the anticancer drug perillyl alcohol in PC12 cells and in the rat. *Toxicol Appl Pharmacol* **167**:55–62.

Cornelissen S, Liu S, Deshmukh AT, Schmid A, Bühler B. 2011. Cell physiology rather than enzyme kinetics can determine the efficiency of cytochrome P450-catalyzed C-H-oxyfunctionalization. *J Ind Microbiol Biotechnol* **38**:1359–1370.

Costerton JW, Lewandowski Z, Caldwell DE, Korber DR, Lappin-Scott HM. 1995. Microbial biofilms. *Annu Rev Microbiol* **49**:711–745.

Duelund L, Amiot A, Fillon A, Mouritsen OG. 2012. Influence of the active compounds of *Perilla frutescens* leaves on lipid membranes. *J Nat Prod* **75**:160–166.

Gibson DG, Young L, Chuang R, Venter JC, Hutchison CA, Smith HO. 2009. Enzymatic assembly of DNA molecules up to several hundred kilobases. *Nat Methods* **6**:343–345.

Gross R, Buehler K, Schmid A. 2013. Engineered catalytic biofilms for continuous large scale production of n-octanol and (*S*)-styrene oxide. *Biotechnol Bioeng* **110**:424–436.

Gross R, Lang K, Bühler K, Schmid A. 2010. Characterization of a biofilm membrane reactor and its prospects for fine chemical synthesis. *Biotechnol Bioeng* **105**:705–717.

Hack CJ, Woodley JM, Lilly MD, Liddell JM. 2000. Design of a control system for biotransformation of toxic substrates: Toluene hydroxylation by *Pseudomonas putida* UV4. *Enzyme Microb Technol* **26**:530–536.

Halan B, Buehler K, Schmid A. 2012. Biofilms as living catalysts in continuous chemical syntheses. *Trends Biotechnol* **30**:453–465.

Halan B, Karande R, Buehler K, Schmid A. 2016. Catalytic *Pseudomonas taiwanensis* VLB120ΔC biofilms thrive in a continuous pure styrene generated by multiphasic segmented flow in a capillary microreactor. *J Flow Chem* **6**:39–42.

Halan B, Schmid A, Buehler K. 2011. Real-time solvent tolerance analysis of *Pseudomonas* sp. strain VLB120ΔC catalytic biofilms. *Appl Environ Microbiol* **77**:1563–1571.

Heipieper HJ, Neumann G, Cornelissen S, Meinhardt F. 2007. Solvent-tolerant bacteria for biotransformations in two-phase fermentation systems. *Appl Microbiol Biotechnol* **74**:961–973.

Hilker I, Baldwin C, Alphand V, Furstoss R, Woodley J, Wohlgemuth R. 2006. On the influence of oxygen and cell concentration in an SFPR whole cell biocatalytic Baeyer-Villiger oxidation process. *Biotechnol Bioeng* **93**:1138–1144.

Inoue A, Horikoshi K. 1989. A *Pseudomonas* thrives in high concentrations of toluene. *Nature* **338**:264–266.

Karande R, Debor L, Salamanca D, Bogdahn F, Engesser K-H, Buehler K, Schmid A. 2016. Continuous cyclohexane oxidation to cyclohexanol using a novel cytochrome P450 monooxygenase from *Acidovorax* sp. CHX100 in recombinant *P. taiwanensis* VLB120 biofilms. *Biotechnol Bioeng* **113**:52–61.

Karande R, Halan B, Schmid A, Buehler K. 2014. Segmented flow is controlling growth of catalytic biofilms in continuous multiphase microreactors. *Biotechnol Bioeng* **111**:1831–1840.

Kurbatov L, Albrecht D, Herrmann H, Petruschka L. 2006. Analysis of the proteome of

Pseudomonas putida KT2440 grown on different sources of carbon and energy. *Environ Microbiol* **8**:466–478.

Lang K, Buehler K, Schmid A. 2015. Multistep synthesis of (*S*)-3-hydroxyisobutyric acid from glucose using *Pseudomonas taiwanensis* VLB120 B83 T7 catalytic biofilms. *Adv Synth Catal* **357**:1919–1927.

Lang K, Zierow J, Buehler K, Schmid A. 2014. Metabolic engineering of *Pseudomonas* sp. strain VLB120 as platform biocatalyst for the production of isobutyric acid and other secondary metabolites. *Microb Cell Fact* **13**:2.

Li XZ, Webb JS, Kjelleberg S, Rosche B. 2006. Enhanced benzaldehyde tolerance in *Zymomonas mobilis* biofilms and the potential of biofilm applications in fine-chemical production. *Appl Environ Microbiol* **72**:1639–1644.

Lima-Ramos J, Neto W, Woodley JM. 2014. Engineering of biocatalysts and biocatalytic processes. *Top Catal* **57**:301–320.

Lindmeyer M, Meyer D, Kuhn D, Bühler B, Schmid A. 2015. Making variability less variable: matching expression system and host for oxygenase-based biotransformations. *J Ind Microbiol Biotechnol* **42**:851–866.

Marques MPC, Cabral JMS, Fernandes P. 2010. Bioprocess scale-up: Quest for the parameters to be used as criterion to move from microreactors to lab-scale. *J Chem Technol Biotechnol* **85**:1184–1198.

Mars AE, Gorissen JPL, van den Beld I, Eggink G. 2001. Bioconversion of limonene to increased concentrations of perillic acid by *Pseudomonas putida* GS1 in a fed-batch reactor. *Appl Microbiol Biotechnol* **56**:101–107.

Mirata MA, Heerd D, Schrader J. 2009. Integrated bioprocess for the oxidation of limonene to perillic acid with *Pseudomonas putida* DSM 12264. *Process Biochem* **44**:764–771.

Panke S, Witholt B, Schmid A, Wubbolts MG. 1998. Towards a biocatalyst for (*S*)-styrene oxide production: characterization of the styrene degradation pathway of *Pseudomonas* sp. strain VLB120. *Appl Env Microbiol* **64**:2032–2043.

Panke S, Meyer A, Huber CM, Witholt B, Wubbolts MG. 1999. An alkane-responsive expression system for the production of fine chemicals. *Appl Environ Microbiol* **65**:2324–2332.

Qureshi N, Annous B a, Ezeji TC, Karcher P, Maddox IS. 2005. Biofilm reactors for industrial bioconversion processes: employing potential of enhanced reaction rates. *Microb Cell Fact* **4**:24.

Schewe H, Mirata MA, Schrader J. 2015. Bioprocess Engineering for Microbial Synthesis and Conversion of Isoprenoids. *Adv Biochem Eng Biotechnol* **123**:127–141.

Schmid C, Steinbrecher R, Ziegler H. 1992. Partition coefficients of plant cuticles for monoterpenes. *Trees* **6**:32–36.

Schmutzler K, Kupitz K, Schmid A, Buehler K. 2016. Hyperadherence of *Pseudomonas taiwanensis* VLB120ΔC increases productivity of (*S*)-styrene oxide formation. *Microb Biotechnol*.

Schmutzler K, Schmid A, Buehler K. 2015. A three-step method for analysing bacterial biofilm formation under continuous medium flow. *Appl Microbiol Biotechnol* **99**:6035–6047.

Segura A, Molina L, Fillet S, Krell T, Bernal P, Muñoz-Rojas J, Ramos JL. 2012. Solvent tolerance in Gram-negative bacteria. *Curr Opin Biotechnol* **23**:415–421.

Sikkema J, de Bont JA, Poolman B. 1995. Mechanisms of membrane toxicity of hydrocarbons. *Microbiol Rev* **59**:201–222.

Singh R, Paul D, Jain RK. 2006. Biofilms: implications in bioremediation. *Trends Microbiol*

14:389–397.

Speelmans G, Bijlsma A, Eggink G. 1998. Limonene bioconversion to high concentrations of a single and stable product, perillic acid, by a solvent-resistant *Pseudomonas putida* strain. *Appl Microbiol Biotechnol* **50**:538–544.

Stark D, von Stockar U. 2003. *In situ* product removal (ISPR) in whole cell biotechnology during the last twenty years. *Adv Biochem Eng Biotechnol* **80**:149–175.

Stewart PS. 2002. Mechanisms of antibiotic resistance in bacterial biofilms. *Int J Med Microbiol* **292**:107–113.

Straathof AJ. 2003. Auxiliary phase guidelines for microbial biotransformations of toxic substrate into toxic product. *Biotechnol Prog* **19**:755–762.

Ütkür FÖ, Gaykawad S, Bühler B, Schmid A. 2011. Regioselective aromatic hydroxylation of quinaldine by water using quinaldine 4-oxidase in recombinant *Pseudomonas putida*. *J Ind Microbiol Biotechnol* **38**:1067–1077.

Walters MC, Roe F, Bugnicourt A, Franklin MJ, Stewart PS. 2003. Contributions of antibiotic penetration, oxygen limitation, and low metabolic activity to tolerance of *Pseudomonas aeruginosa* biofilms to ciprofloxacin and tobramycin. *Antimicrob Agents Chemother* **47**:317–323.

Warikoo V, Godawat R, Brower K, Jain S, Cummings D, Simons E, Johnson T, Walther J, Yu M, Wright B, Mclarty J, Karey KP, Hwang C, Zhou W, Riske F, Konstantinov K. 2012. Integrated continuous production of recombinant therapeutic proteins. *Biotechnol Bioeng* **109**:3018–3029.

Willrodt C, Karande R, Julsing MK, Schmid A. 2015. Guiding efficient microbial synthesis of non-natural chemicals by physicochemical properties of reactants. *Curr Opin Biotechnol* **31**:52–62.

Wohlgemuth R, Plazl I, Žnidaršič-Plazl P, Gernaey K V., Woodley JM. 2015. Microscale technology and biocatalytic processes: opportunities and challenges for synthesis. *Trends Biotechnol* **33**:302–314.

Wolff JA, MacGregor CH, Eisenberg RC, Phibbs P V. 1991. Isolation and characterization of catabolite repression control mutants of *Pseudomonas aeruginosa* PAO. *J Bacteriol* **173**:4700–4706.

Woodley JM. 2008. New opportunities for biocatalysis: making pharmaceutical processes greener. *Trends Biotechnol* **26**:321–327.

Xue R, Woodley JM. 2012. Process technology for multi-enzymatic reaction systems. *Bioresour Technol* **115**:183–195.

Figure Legends

Figure 1: Schematic representation of the segmented flow biofilm reactor (**A**) and the reaction scheme for the multi-step bioconversion of (*R*)-(+)-limonene to (*R*)-(+)-perillic acid (**B**). The silicon membrane biofilm reactor is supplied with fresh minimal medium and air via Tygon tubes using peristaltic pumps. Consecutive air/liquid segments are generated by applying a T-connector. Limonene is supplied from a sealed reservoir to minimize substrate evaporation by diffusion through the silicon membrane. A cross-section close-up view illustrates the biofilm attachment to the membrane and the air/aqueous segmented flow. Abbreviations: CymA (*p*-cymene monooxygenase), CymB (*p*-cumic alcohol dehydrogenase), CymC (*p*-cumic aldehyde dehydrogenase), DH (dehydrogenases), (*R*)-(+)-limonene (**1**), (*R*)-(+)-perillyl alcohol (**2**), (*R*)-(+)-perillyl aldehyde (**3**), (*R*)-(+)-perillic acid (**4**). The figure was adapted from Karande and co-workers (Karande et al., 2014).

Figure 2: Biomass-specific production of oxygenated limonene products during a resting cell assay with *P. taiwanensis* VLB120 harboring either pCom10L:CymA (**A**) or pCom10L:CymAB (**B**) from 2 mM (*R*)-(+)-limonene. Cells were harvested four hours after induction of gene expression with 1 mM IPTG. Concentrations of perillic acid (■), perillyl aldehyde (♦), and perillyl alcohol (▲) were assessed by GC. After the cells were incubated in minimal medium with citrate, the resting cell assays were performed in 0.1 M potassium phosphate buffer (pH 7.4) at 30°C and orbital shaking. The error bars were retrieved from standard deviations of two independent cultivations and assays (biological duplicates).

Figure 3: Effect of varying limonene (**A**) and perillic acid (**B**) concentration on the final biomass yield of *P. taiwanensis* VLB120 (■) and *P. putida* GS1 (●). Different concentrations of the compounds were added directly after inoculation. For the limonene toxicity evaluation, the gaseous phase was saturated with limonene via an evaporation container to avoid limonene loss.

Experiments were carried out in M9* with citrate as sole carbon and energy source and the error bars refer to standard deviations obtained from two independent cultivations (biological duplicates).

Figure 4: Evaluation of biofilm formation capacity of *P. taiwanensis* VLB120 (grey bars) and *P. putida* GS1 (white bars) (**A**). The biofilm dry weight was assessed after cultivation of the respective strain with glycerol, glucose, or citrate (0.5% (w/v) under single-phase continuous flow (0.1 ml min^{-1}) for two days. The error bars refer to standard deviations obtained from three independent cultivations (biological triplicates). Panel **B** shows a photographic image of the freshly harvested biofilm of either of *P. taiwanensis* VLB120 and *P. putida* GS1 cultivated with citrate as sole carbon and energy source.

Figure 5: Synthesis of (*R*)-(+)-perillic acid in a segmented flow biofilm reactor with *P. putida* GS1 (**A**) and *P. taiwanensis* VLB120 (pCom10L:CymAB) (**B)** using either glycerol (●) or citrate (■) as carbon source. A single-phase flow of 0.1 mL min^{-1} was applied during the first two days after inoculation. Subsequently, the air flow was started at a flow rate of 0.4 mL min^{-1} (as indicated by the arrow). The (*R*)-(+)-perillic acid concentration was assessed by GC after regular sampling from the outlet of the 1 m reactor. The error bars refer to standard deviations from at least two independent biofilm experiments.

Tables

Table 1: Summary of the process performance for the biofilm-based production of perillic acid in a segmented-flow reactor.

Host strain	carbon source	Operation time of the biofilm reactor/ d	Max. product concentration/ mg L^{-1}	Max. volumetric productivity/ g L^{-1} d^{-1}	Max. surface area-based productivity/ g m^{-2} d^{-1}
P. putida GS1 (DSM 12264)	glycerol	12	870	33.8	5.5
	citrate	12	157	6.1	1.0
P. taiwanensis VLB120 (pCom10L:CymAB)	glycerol	12	82	3.2	0.5
	citrate	12	62	2.6	0.4

Figures

Figure 1

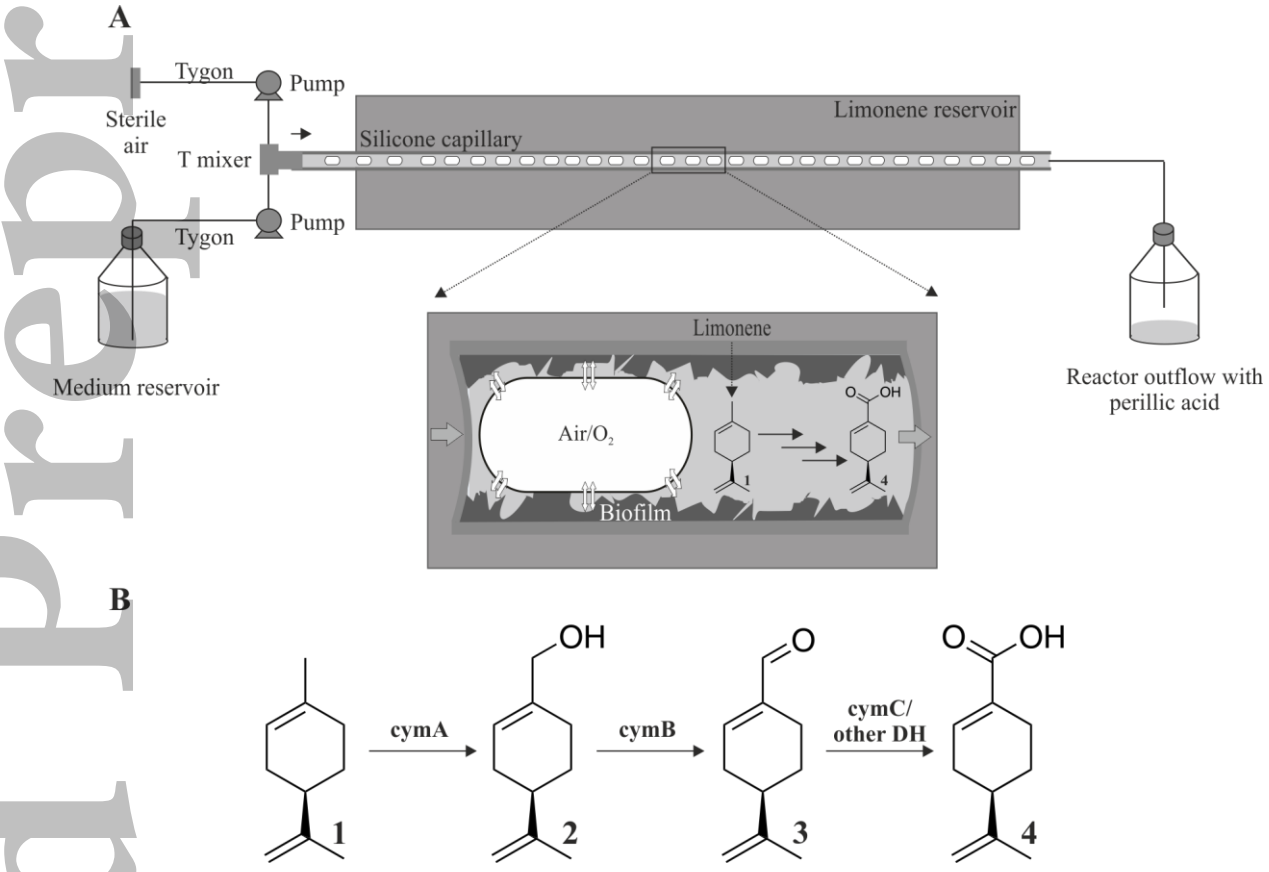

Figure 2

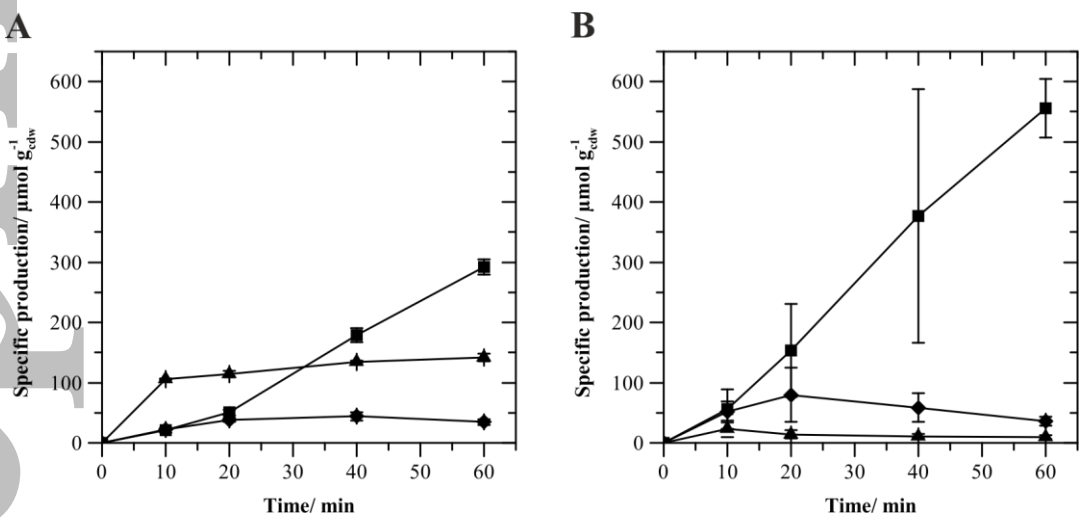

Figure 3

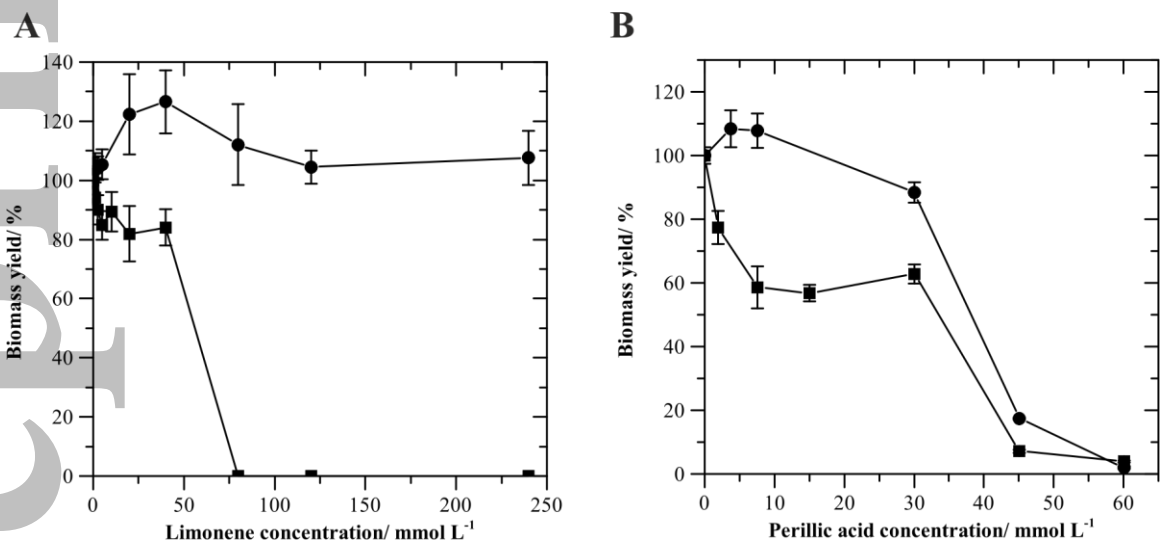

Figure 4

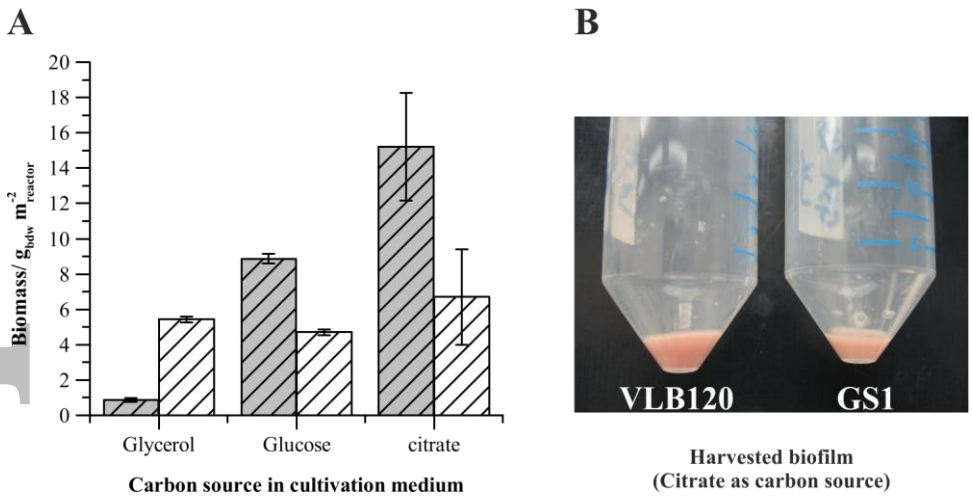

Figure 5